eprints@whiterose.ac.uk
https://eprints.whiterose.ac.uk/

Journal Name

ARTICLE

Highly selective detection of Hg^{2+} and MeHgI by di-pyridin-2-yl-[4-(2-pyridin-4-yl-vinyl)-phenyl]-amine and its zinc coordination polymer

Min-Min Chen,[ab] Liang Chen,[a] Hong-Xi Li,*[a] Lee Brammer*[c] and Jian-Ping Lang*[ab]

Solvothermal reaction of Zn(NO$_3$)$_2$·6H$_2$O with di-pyridin-2-yl-[4-(2-pyridin-4-yl-vinyl)-phenyl]-amine (ppvppa) and 1,4-naphthalenedicarboxylic acid (1,4-H$_2$NDC) in H$_2$O and MeCN at 150 °C yielded a two-dimensional (2D) coordination Zn(II) polymer [Zn(ppvppa)(1,4-NDC)]$_n$ (**1**). Compound **1** was characterized by elemental analysis, IR spectroscopy, powder X-ray diffraction, single-crystal X-ray diffraction and thermogravimetric analysis. Compound **1** consists of dimeric [Zn$_2$(ppvppa)$_2$] units linked by 1,4-NDC bridges to generate a 2D honeycomb network. Either compound **1** or ppvppa alone can detect Hg^{2+} or MeHgI selectively and with good sensitivity. Upon addition of Hg^{2+} ions to a MeCN solution of ppvppa, marked changes in the UV-vis and fluorescence spectra are observed, associated with colour changes, which are easily identified by the naked eye. The pyridinyl rings of ppvppa are coordinated to the Hg^{2+} ion. This motif in the presence of NO$_3^-$ ions forms a binuclear complex [Hg$_2$(ppvppa)$_2$(NO$_3$)$_4$] (**2**), which has been characterized as the solvate [Hg$_2$(ppvppa)$_2$(NO$_3$)$_4$]·H$_2$O·4MeCN (**2**·H$_2$O·4MeCN) by single-crystal X-ray diffraction studies. In aqueous solution, compound **1** emits pale orange light at ambient temperature and the addition of Hg^{2+} or MeHgI induces an change of fluorescence color from pale orange to blue. Compound **1** is a promising candidate as a sensitive naked-eye indicator for Hg^{2+} or MeHgI in water under a UV lamp.

Introduction

Divalent mercury ions are highly toxic to the environment and to human beings due to bioaccumulation and long residence, which can lead to permanent deterioration in health. In particular, the methylation of mercury enhances its lipid solubility, and methylated mercury is extremely detrimental to the central nervous system.[1-7] Therefore, the development of practical analytical methods for highly selective and sensitive detection of Hg^{2+} and MeHg$^+$ ions in the environment, medicine, biology and food remains an urgent issue to be addressed.[8,9] Several detection techniques for Hg^{2+} ions mainly rely on gas chromatography, atomic absorption spectroscopy, and cold vapour atomic fluorescence spectrometry, which are time-consuming, costly, and may not be easily accessible in most cases.[10-13] Fluorescence-based techniques for sensing Hg^{2+} provide a promising approach for simple and rapid tracking of mercury ions in biological, toxicological and environmental monitoring.[8,14-18] A large number of highly sensitive and selective "turn-on" or "turn-off" fluorescent probes for Hg^{2+} have been reported.[19-26] These single intensity-based detectors are usually compromised by other metal ions, the concentration change of sensors, drift of light source, and environmental effects.[27] In this regard, ratiometric fluorescence chemosensors are attractive candidates for the detection of mercury ions. Such sensors undergo a color change in response to the analyte, with the change in emission wavelength correlated to analyte concentration, enabling quantitative detection. The shift in the emission can overcome the disturbances induced by environmental fluorescence to improve the selectivity and sensitivity.[28-35] Although a variety of fluorescent ratiometric sensors for Cu^{2+}, Fe^{3+}, etc. have been documented,[36-42] only a few ratiometric Hg^{2+} probes have been reported to date.[43-46] Therefore it remains a challenge to develop a highly effective fluorescent Hg^{2+} sensor. Various pyridine-appended π-conjugated derivatives have proved to be highly selective and sensitive as chemosensors for transition metal ions.[47-54] Very recently, we have been interested in the syntheses and structures of metal coordination polymers and their detection of toxic compounds.[55-57] For this purpose we designed di-pyridin-2-yl-[4-(2-pyridin-4-yl-vinyl)-phenyl]-amine (ppvppa) with one extended π-conjugated core.[55] Its Cd complex {Cd(ppvppa)(1,4-NDC)}$_n$ (1,4-H$_2$NDC = 1,4-

a. State and Local Joint Engineering Laboratory for Novel Functional Polymeric Materials, College of Chemistry, Chemical Engineering and Materials Science, Soochow University, Suzhou 215123, Jiangsu, People's Republic of China, Email: jplang@suda.edu.cn, lihx@suda.edu.cn.
b. State Key Laboratory of Organometallic Chemistry, Shanghai Institute of Organic Chemistry, Chinese Academy of Sciences, Shanghai 200032, People's Republic of China.
c. Department of Chemistry, University of Sheffield, Brook Hill, Sheffield S3 7HF, UK, Email: lee.brammer@sheffield.ac.uk

naphthalenedicarboxylic acid; λ_{em} = 478 nm) exhibits a red emission shift of about 60 nm relative to the uncoordinated ppvppa ligand (λ_{em} = 418 nm), and has been effective in sensing nitroaromatics.[55] The shift in fluorescence emission presents an opportunity to develop an easy assay for the ratiometric detection of metal ions by binding to the di(pyridine-2-yl)amine chelating site of ppvppa. In support of this proposal, we have previously reported the coordination polymers [M(ppvppa)$_2$(1,3-BDC)] (M = Cd, Co; 1,3-H$_2$BDC = isophthalic acid) which forms with the di(pyridine-2-yl)amine chelating site uncoordinated.[58] Exposure of the coordination polymer to a solution containing Ag$^+$ ion results in a red shift of the fluorescence emission band, suggesting coordination to the chelating site. In the present study our interest is in whether coordination complexes of ppvppa with an uncoordinated di(pyridine-2-yl)amine chelating site can selectively detect mercury ions with high sensitivity through coordination of the Hg^{2+} ions at this binding site. With this in mind, we carried out the reaction of Zn(NO$_3$)$_2$·6H$_2$O with 1,4-H$_2$NDC and ppvppa to form the two-dimensional coordination polymer [Zn(ppvppa)(1,4-NDC)]$_n$ (1), which exhibits highly selective detection of MeHgI and Hg^{2+} in aqueous media. The ppvppa ligand can also be used as a colorimetric and ratiometric fluorescence sensor for Hg^{2+} in MeCN.

Results and discussion

Synthesis and crystal structure of [Zn(ppvppa)(1,4-NDC)]$_n$ (1).

Solvothermal reaction of Zn(NO$_3$)$_2$·6H$_2$O with 1,4-H$_2$NDC and ppvppa (molar ratio = 2:1:2) in H$_2$O/MeCN (v/v = 1/1) at 150 °C afforded yellow crystals of 1 in 18% yield. The reaction solvent and temperature had a significant influence on the formation of 1. When we carried out the analogous reactions of the same components in other solvents such as EtOH/MeCN and H$_2$O/EtOH, only a large amount of insoluble precipitates were observed. When a similar reaction was carried out at a higher temperature (e.g. 170 °C), the same product 1 was generated in a lower yield. Intriguingly, when we raised the ratio of H$_2$O/MeCN (v/v) from 1:1 to 2:1, 1 was obtained in a higher yield (87%). For the same components Zn(NO$_3$)$_2$·6H$_2$O/1,4-H$_2$NDC/ppvppa, similar reactions at ambient temperature did not give rise to the product 1. Compound 1 is stable in air and insoluble in water and common organic solvents such as CHCl$_3$, CH$_3$CN, CH$_3$OH and DMF. It gives satisfactory elemental analysis and its powder X-ray diffraction (PXRD) patterns closely resemble those generated from the single-crystal X-ray structure (Fig. S1, ESI†), suggesting a phase-pure material. The IR spectrum of 1 exhibits strong bands for stretching vibrations at 1510–1600 cm^{-1} and 1330–1469 cm^{-1}, which are assignable to the coordinated carboxyl group. High thermal stability is an essential requirement for practical applications. Thermogravimetric analysis (TGA) of 1 (Fig. S2, ESI†) confirmed that complex 1 is stable upon heating up to 330 °C.

Single crystal X-ray analysis reveals that 1 crystallizes in the triclinic space group $P\bar{1}$ and its asymmetric unit contains one {Zn(ppvppa)(1,4-NDC)} unit. Each Zn(II) centre is tetrahedrally coordinated by two O atoms from two 1,4-NDC ligands and

two N atoms from two ppvppa ligands (Fig. 1a). Two Zn atoms are bridged by two ppvppa ligands to form a [Zn$_2$(ppvppa)$_2$] unit (Fig. 1a). The resulting [Zn$_2$(ppvppa)$_2$] unit is interlinked to other equivalent ones by four 1,4-NDC bridges to generate a 2D honeycomb network (Fig. 1b). As shown in Fig. 1b, one of two pyridyl rings on the dipyridinylamine group in 1 remains uncoordinated, suggesting it may bind extra metal ions like Hg^{2+} through M–N coordination.
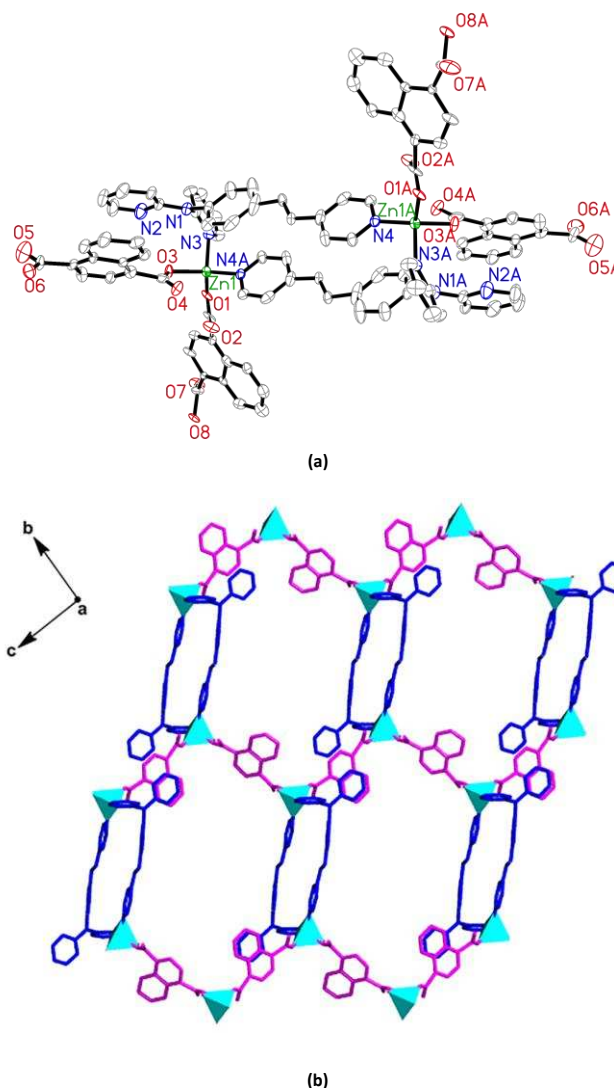

(a)

(b)

Fig. 1 (a) View of the {Zn$_2$(ppvppa)$_2$(1,4-NDC)$_4$} fragment in 1. Atoms represented with 30% displacement ellipsoids; H atoms are omitted along with second component of disordered ligands, for clarity. Selected bond lengths (Å): Zn1-O1 2.00(4), Zn1-O3 1.897(17), Zn1-N3 2.109(4), Zn1-N4A 2.006(3). Symmetry code: (A) − x + 1, − y + 1, − z. (b) View down the a-axis of the 2D network of 1, which extends in the bc plane.

Hg^{2+} colorimetric and ratiometric fluorescent sensing properties of ppvppa

The recognition of metal ions by ppvppa was investigated by UV–vis absorption spectroscopy. Accordingly, the experiment was performed in a MeCN solution containing ppvppa as the probe at a concentration of 0.1 mmol L^{-1}. In the absence of any metal ions, the absorption spectrum of ppvppa is characterized by three intense bands centered at 245 nm, 273

nm, and 311 nm (Fig. 2a). Almost no absorption in the visible region (above 400 nm) was observed. These absorption bands are probably derived from the intraligand π→π* or n→π* transitions.[51,59] Variation of the absorption spectrum of ppvppa upon addition of 1 equiv. of different metal ions such as Na$^+$, K$^+$, Zn^{2+}, Co^{2+}, Ni^{2+}, Cu^{2+}, Cd^{2+}, Mn^{2+}, Pb^{2+}, Hg^{2+} and MeHgI (0.1 mmol L^{-1}) is shown in Fig. 2a. Upon addition of Hg^{2+}, new absorption bands near 380 nm appear. Formation of the new bands confirms the interaction of Hg^{2+} ions with the nitrogen atom of pyridine groups of ppvppa, which leads to intramolecular charge transfer from the π-conjugated core to the coordinating N atom.[60-63] By contrast, little change in the absorption was observed and no new bands were formed upon addition of Na$^+$, K$^+$, Zn^{2+}, Co^{2+}, Ni^{2+}, Cu^{2+}, Cd^{2+}, Mn^{2+} Pb^{2+} or MeHgI. As shown in Fig. 2b, the addition of increasing amounts of Hg^{2+} (from 0 to 34 ppm) to the ppvppa solution led to a gradual blue shift of the absorption band centered at 311 nm with the concomitant increase in a new band at around 380 nm. Correspondingly, in the presence of mercury ions, the colour of the ppvppa solution changed from colourless to yellow, which is witnessed easily by eye (Fig. 2c). The drastic colour change indicates that ppvppa can be applied as a sensitive naked-eye colorimetric chemosensor for Hg^{2+} ions.
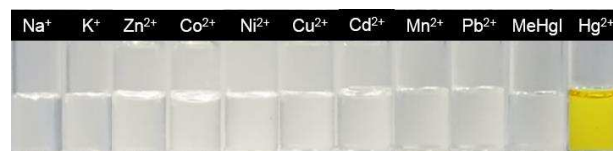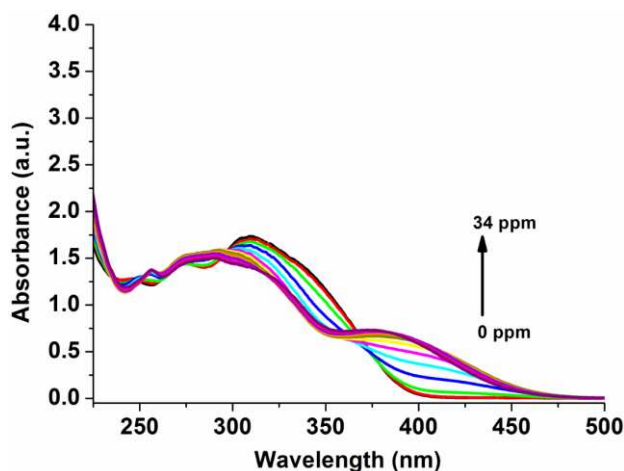

(c)

Fig. 2 (a) Absorbance spectra change of ppvppa (0.1 mmol L^{-1}) upon addition of different metal ions (1 equiv.) in MeCN solution. (b) Absorbance spectra of ppvppa (0.1 mmol L^{-1}) in the presence of increasing Hg^{2+} concentrations (0-34 ppm) in MeCN solution. (c) The colours of the solutions containing ppvppa with different metal ions.

Fluorescence spectroscopic analyses were performed to scrutinize the sensing property of the chemoprobe. Fluorescence intensity measurements for ppvppa were carried out in MeCN. Upon excitation at 405 nm, ppvppa shows a single fluorescence band with maximum at around 460 nm. With increasing addition of Hg^{2+} (from 0 to 18 ppm), the original emission at 460 nm was gradually quenched concurrent with the sharp growth of a new peak at 580 nm, i.e. a large emission red-shift of about 120 nm (Fig. 3a). The limit of detection for ppvppa was found to be 0.58 ppm for Hg^{2+} on the basis of the signal to noise ratio of 3 (limit of detection = 3×SD/S). This indicates that ppvppa might serve as a dual-signal Hg^{2+}-selective fluorescent ratiometric chemoprobe. Other metal ions (Na$^+$, K$^+$, Zn^{2+}, Co^{2+}, Ni^{2+}, Cu^{2+}, Cd^{2+}, Mn^{2+}, Pb^{2+} and MeHgI) were examined as controls under the same conditions.
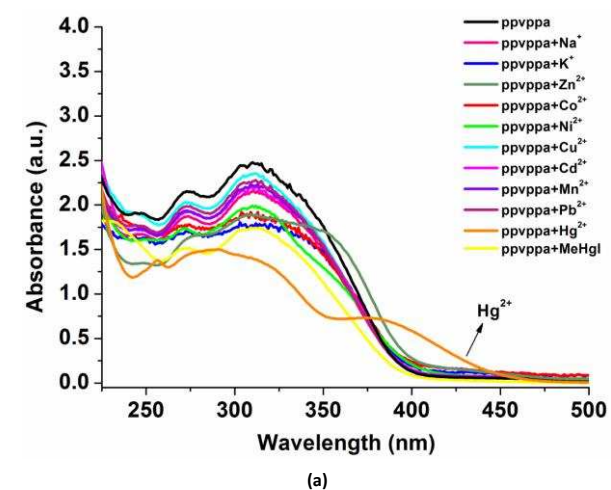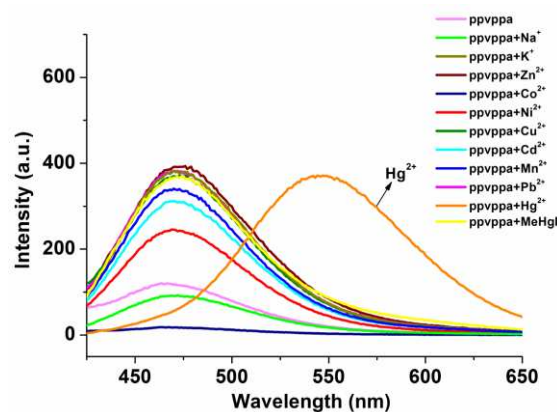

(a)
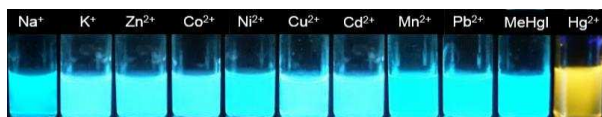

(b)
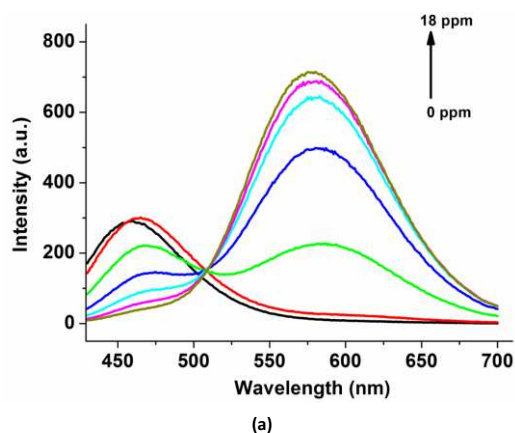
(a)


(b)

(c)

Fig. 3 (a) Emission spectra of ppvppa (0.1 mmol L^{-1}) in the presence of increasing Hg^{2+} concentrations (0-18 ppm) in MeCN. (b) Emission spectra change of ppvppa (0.1 mmol L^{-1}) upon addition of different metal ions (1 equiv.) in MeCN. Excitation wavelength was 405 nm. (c) Colours of the solutions containing ppvppa with different metal ions under UV light.

As shown in Fig. 3b, the presence of K^+, Zn^{2+}, Ni^{2+}, Cu^{2+}, Cd^{2+}, Mn^{2+}, Pb^{2+} or MeHgI enhances the luminescence intensity with no significant change in emission wavelength. In contrast, Na^+ and Co^{2+} resulted in luminescence quenching. The large ion-induced bathochromic shift for Hg^{2+} in the emission spectrum resulted in a colour change from blue to yellow under UV light. This clearly visible emission allows Hg^{2+} to be distinguished by the naked eye (Fig. 3c). To determine whether ppvppa acts as a highly selective luminescent sensor for Hg^{2+}, its detection selectivity and its sensing ability in the presence of competitor ions was investigated. Typically, Na^+, K^+, Zn^{2+}, Co^{2+}, Ni^{2+}, Cu^{2+}, Cd^{2+}, Mn^{2+}, or Pb^{2+} ions (each 10 μmol L^{-1}) were added into separate MeCN solutions of ppvppa (5 μmol L^{-1}) under the same conditions. As shown in Fig. 4, little variation in emission intensity for ppvppa ($0.1 < I_{580\,nm}/I_{460\,nm} < 0.3$) was observed in the presence of each of the competitor ions. When Hg^{2+} ions were added into the solutions containing one of the metal ions, the value of the fluorescence ratios ($I_{580\,nm}/I_{460\,nm}$) increased drastically by a factor of 12-38. These results show that the Hg^{2+} ion has much greater affinity for ppvppa than other metal ions. Therefore the ppvppa sensor exhibits a high sensitivity and selectivity in the detection of Hg^{2+}.
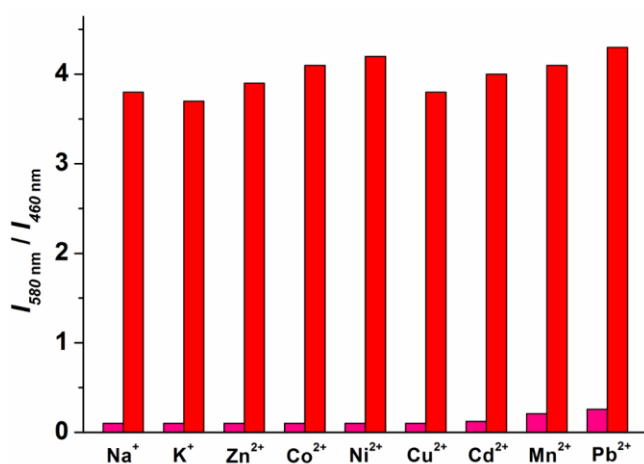

Fig. 4 Fluorescence response of ppvppa (5 μM) in the presence of Hg^{2+} ions (5 μM) with various other metal ions (10 μM) in MeCN. The bars represent the fluorescence intensity ratio at λ = 460 nm and 580 nm ($I_{580\,nm}/I_{460\,nm}$) when λ_{ex} = 405 nm. Pink bars: each metal ion was added. Red bars: Hg^{2+} was added together with each metal ion.

Slow evaporation of a MeCN solution of ppvppa and $Hg(NO_3)_2$ gave rise to yellow crystals of the binuclear cyclic compound $[Hg_2(ppvppa)_2(NO_3)_4] \cdot H_2O \cdot 4MeCN$ (**2**·H_2O·4MeCN). Complex **2** crystallizes as its solvate **2**·H_2O·4MeCN in the

triclinic space group $P\bar{1}$ and its asymmetric unit contains one-half of the discrete molecule $Hg_2(ppvppa)_2(NO_3)_4$, one-half of H_2O and two MeCN solvent molecules. Each Hg(II) centre is coordinated by two O-atoms from different NO_3^- ions and two N-atoms from different ppvppa ligands, forming a seesaw-shaped coordination geometry. Two $\{Hg(NO_3)_2\}$ fragments are bridged by two ppvppa ligands in a head-to-tail manner to form a binuclear metallocyclic structure (Fig. 5). In **2**, the distance across the macrocycle between the phenyl ring and vinyl group is about 3.6 Å, which indicates strong π-π interaction.
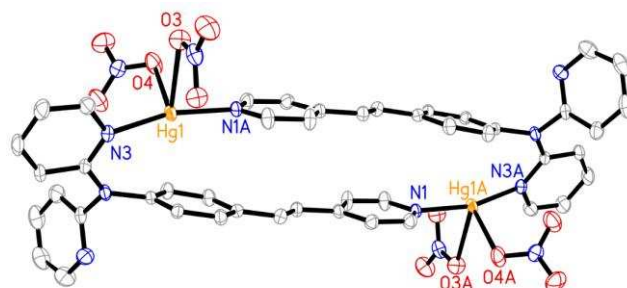
Fig. 5 View of the molecular structure of **2**, shown with atoms represented as 30% displacement ellipsoids. All H atoms were omitted for clarity. Selected bond lengths (Å) and angles (°) for **2**: Hg1-O3 2.600(5), Hg1-O4 2.465(5), Hg1-N1A 2.135(5), Hg-N3 2.135(5), N1A-Hg1A-N3 164.9(2). Symmetry code: (A) $-x + 2, -y, -z + 1$.
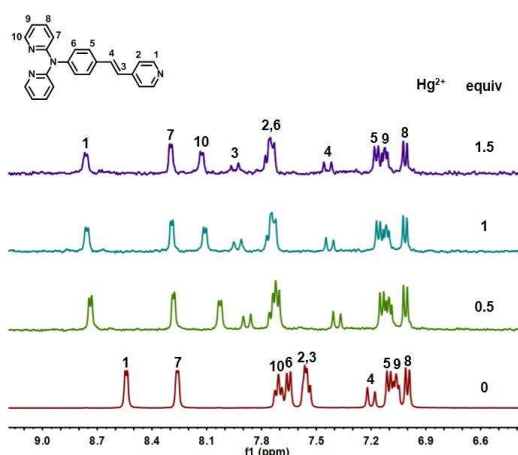
Fig. 6 ^1H NMR titration of ppvppa with $Hg(NO_3)_2$ in DMSO-d_6 solution.

A ^1H NMR titration was performed to elucidate more detailed information on the complexation of Hg^{2+} with ppvppa in DMSO-d_6. Stacked spectra recorded for ppvppa in the presence of increasing Hg^{2+} (0-1.5 equiv.) are shown in Fig. 6. The addition of Hg^{2+} led to a significant downfield shift for the signals of the protons (H_1, H_{10} and H_2) of the pyridyl ring from δ 8.54, 7.71, 7.55 to 8.76, 8.12, 7.75, which indicates that the N atoms of ppvppa are involved in the coordination at Hg^{2+}. In particular, the shift is greater for H_{10} than that for H_1 and H_2, when the two equivalent H_{10} sites are accounted for, which might suggest that Hg^{2+} binding is primarily at the chelating site with less binding occurring at the lone pyridyl site. The chemical shift of the protons (H_3 and H_4) on the vinyl group and the protons (H_6) of the phenyl group also underwent a

downfield shift from δ 7.55, 7.20 to 7.95, 7.44, and from δ 7.65 to 7.75, respectively. The changes in the ^{1}H NMR spectra upon titration with Hg^{2+} showed that saturation of the change in chemical shift for ppvppa protons occurred when 1 equiv of Hg^{2+} ion was added, which suggests a 1 : 1 stoichiometry of the complex between ppvppa and Hg^{2+} ion. The coordination of Hg^{2+} ions caused a downfield chemical shift of the protons of the pyridine rings, vinyl and phenyl groups in ppvppa. These phenomena confirm that Hg^{2+} interacts with the nitrogen atom on the ppvppa ligand, which causes the intramolecular charge transfer and the fluorescence emission red shift.

Hg^{2+} and MeHgI fluorescent sensing properties of coordination polymer, 1

The finding that ppvppa can serve as a ratiometric chemosensor for Hg^{2+} encouraged us to further explore the sensing applications of the coordination polymer, **1**. Consequently, the photoluminescent properties of **1** in the solid state and in aqueous suspension at room temperature were investigated. The excitation and emission spectra of **1** in the solid state were recorded (Fig. 7). Compound **1** exhibits a strong emission at 508 nm when excited at 419 nm. As discussed above, the uncoordinated dipyridinylamine groups in **1** may be used as the potential ionophoric receptor for Hg^{2+} or $MeHg^+$ ions. Accordingly, we investigated the fluorescent **1** for the possible detection of Hg^{2+} or $MeHg^+$ ions in water. In order to identify the potential of **1** for sensing of metal ions, finely-ground samples of **1** were soaked in aqueous solutions of 1 mmol L^{-1} $M(NO_3)_n$ (M = Na^+, K^+, Zn^{2+}, Co^{2+}, Ni^{2+}, Cu^{2+}, Cd^{2+}, Mn^{2+}, Pb^{2+}, and Hg^{2+}) or MeHgI to give the metal-ion-incorporated suspensions of **1** for luminescence measurements. As shown in Fig. 8a, emission intensities of the different suspensions is strongly dependent on the incorporated metal ions. When immersed in an aqueous solution of Na^+, K^+, Zn^{2+}, Co^{2+}, Ni^{2+}, Cu^{2+}, Cd^{2+}, Mn^{2+}, or Pb^{2+} ions, emission maxima of similar intensity were observed at 503 nm and 595 nm, upon excitation at 370 nm. The resultant pale orange fluorescence of **1** shows no significant variation in colour with these metal ions (Fig 8b). When **1** was dispersed in aqueous solutions of Hg^{2+} or MeHgI an enhanced emission of the higher energy maximum, which is slightly blue-shifted at 494 nm, accompanied by a decrease of the fluorescence intensity of the emission at 595 nm leads to a change of fluorescence colour from pale orange to blue (Fig. 8b). These results suggest that complex **1** could serve as a sensitive naked-eye indicator for Hg^{2+} or MeHgI under UV light. With increasing addition of Hg^{2+} (0-0.4 ppm) or MeHgI (0-0.3 ppm), the intensity of the emission peak at 494 nm gradually increases (Fig 9). A good linear correlation (R^2 = 0.94 for Hg^{2+} or R^2 = 0.98 for MeHgI) exists between the fluorescence intensity and the concentration of Hg^{2+} in the range of 0.02–0.17 ppm or MeHgI in the range of 0.06–0.21 ppm (Fig. S3, ESI†). The detection limit for **1** was calculated to be 0.02 and 0.06 ppm for Hg^{2+} and MeHgI, respectively. For the X-ray photoelectron spectra (XPS) of **1** and the sample derived from **1** dispersed in an aqueous solution of Hg^{2+} ions, the Zn $2p_{3/2}$ and Zn $2p_{1/2}$ peaks at 1021.6 eV and 1044.8 eV, respectively, were

unchanged, suggesting that Zn retains its original coordination environment. However, the latter material showed peaks at 359.6 eV and 378.3 eV are assignable to the Hg $4d_{5/2}$ and Hg $4d_{3/2}$, which are consistent with those reported for known Hg(II) complexes.[64] (Fig. S4, ESI†). Inductively coupled plasma optical emission spectrometry (ICP-OES) analyses of **1** immersed into Hg^{2+} solution after the detection have been measured. The analysis revealed that the ratio of Zn^{2+} and Hg^{2+} is approximately 1.04 : 0.69. To this end, we assumed that Hg^{2+} ions are doped onto the network of **1** *via* their interactions with the unsaturated N atoms. Thus, **1** exhibits relatively high selectivity towards Hg^{2+} detection through its binding at the (chelating) pyridyl site.

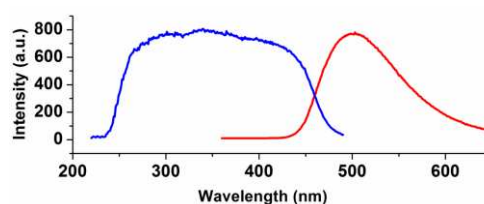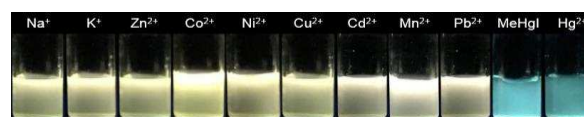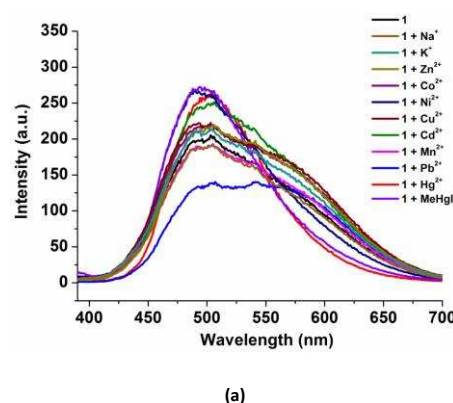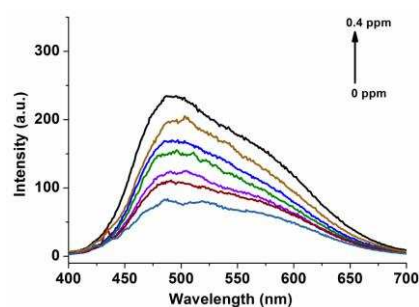
Fig. 7 The excitation (left) and emission (right) spectra of **1** in the solid state at ambient temperature.

(a)
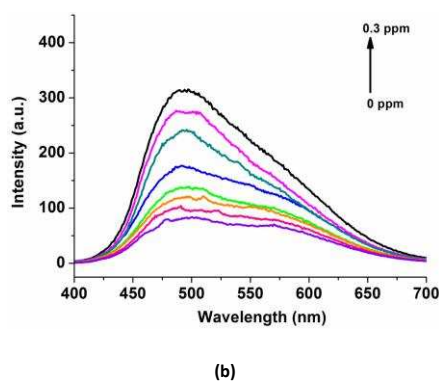

(b)

Fig. 8 (a) The emission spectra of **1** in H_2O and **1** immersed in the solutions containing different metal ions (1 mmol·L^{-1}); excitation wavelength was 370 nm. (b) The colour of the suspensions of **1** with different metal ions under UV light.

(a)

Fig. 9 Emission spectra of **1** (0.1 mmol L^{-1}) in the presence of increasing concentrations of (a) Hg^{2+} (0-0.4 ppm); (b) MeHgI (0-0.3 ppm) in H_2O.

Conclusions

In summary, the assembly of Zn(II) ions and ppvppa yielded a robust 2D coordination polymer **1**. Each ppvppa ligand in **1** adopts a μ,κ_1-N,κ_1-N' coordination mode to link two Zn atoms, forming a [Zn_2(μ-ppvppa)$_2$] cyclic unit. These units are connected by 1,4-NDC ligands to form a 2D honeycomb network. Complex **1** and ppvppa can be used for the "naked-eye" detection of Hg^{2+} or MeHgI with high selectivity and sensitivity. For ppvppa, both the colour and fluorescence changes are remarkably specific for Hg^{2+}. The colour of the ppvppa solution turned from colourless to yellow upon incremental addition of Hg^{2+} ion. The fluorescence emission maximum of ppvppa is red-shifted with the addition of Hg^{2+}, which causes a colour change from blue to yellow under UV light. The structure of **2** suggested a possible 1:1 binding for ppvppa-Hg^{2+} consistent with solution-phase titrations. The addition of Hg^{2+} or MeHgI to an aqueous suspension of **1** induces a fluorescent color change from pale orange to blue. The noticeable change in the fluorescence colour can be observed by eye with ease under UV light. These detection methods are very convenient and fast. It is anticipated that the luminescent coordination polymers with pyridine-appended π-conjugated derivatives may be rationally designed to serve as practical highly-responsive sensors for the detection of heavy metal ions in water. Such studies are currently underway in our laboratory.

Experimental

Materials and methods

General Procedure.

Ligand ppvppa was prepared according to the published procedure.[11] Metal nitrates, acetonitrile, MeHgI and 1,4-H_2NDC were obtained from Sinopharm Chemical Reagent Co., Ltd., Strem Chemicals, Inc., and Tokyo Chemical Industry Co., Ltd and used as received. The flash column chromatography was carried out on silica gel (300-400 mesh). Elemental analyses (CHN) were performed on a Carlo-Erba CHNO-S microanalyzer. Infrared spectra were obtained (KBr disk, 400–4000 cm^{-1}) on a Perkin-Elmer Model 1320 spectrometer.

The ^{1}H NMR spectra in DMSO-d_6 were recorded at ambient temperature on a Varian UNITY plus-400 spectrometer. The ^{1}H NMR chemical shifts were referenced to the solvent signal in DMSO-d_6. Thermogravimetric analysis (TGA) was obtained on a Mettler Toledo Star System (heating rate of 5 °C/min). The powder X-ray diffraction (PXRD) measurements were carried out on a PANalytical X'Pert PRO MPD system (PW3040/60). X-ray photoelectron spectra (XPS) were recorded on a Thermo-Fisher Scientific ESCALAB 250Xi X-ray photoelectron spectrometer (with Al Kα X-ray radiation as the X-ray source for excitation, whose binding energies were referenced to C 1s at 284.7 eV from hydrocarbon to compensate charging effect). The UV-Vis absorption spectra were measured on a Varian Cary-50 UV-visible spectrophotometer. The photoluminescence spectra were obtained on a Perkin-Elmer LS55 spectrofluorometer or a Varian Cary-Eclipse fluorescence spectrophotometer.

Preparation of [Zn(ppvppa)(1,4-NDC)]$_n$ (1). A mixture of $Zn(NO_3)_2$·6H_2O (5 mg, 0.02 mmol), 1,4-H_2NDC (2 mg, 0.01 mmol) and ppvppa ligand (7 mg, 0.02 mmol) in 2 mL of H_2O and 1 mL of MeCN was sealed in a glass tube and heated under autogenous pressure to 150 °C for 24 h. Cooling to room temperature at the rate of 5 °C per hour yielded yellow crystals of **1**, which were collected by filtration, washed with EtOH and dried *in vacuo*. Yield: 5.5 mg (87% based on 1,4-H_2NDC). Anal. Calcd. for $C_{35}H_{24}ZnN_4O_4$: C, 66.73; H, 3.84; N, 8.89%. Found: C, 66.58; H, 3.76; N, 9.35%. IR (KBr disk, cm^{-1}): 3063 (m), 1600 (s), 1510 (m), 1469 (m), 1434 (s), 1400 (s), 1330 (s), 1259 (m), 834 (m), 783 (m) cm^{-1}.

Preparation of [Hg$_2$(ppvppa)$_2$(NO$_3$)$_4$]·H_2O·4MeCN (2·H_2O·4MeCN). A solution of $Hg(NO_3)_2$·H_2O (3.42 mg, 0.01 mmol) and ppvppa (3.51 mg, 0.01 mmol) in MeCN (4 mL) was stirred for *ca.* 1 h to form a yellow solution at room temperature. The solution was filtered and slow diffusion of Et$_2$O into the filtrate for several days afforded yellow crystals of **2·H_2O·4MeCN**, which were collected by filtration, washed with MeOH, and dried *in vacuo*. Yield: 2.2 mg (29% based on Hg). Anal. Calcd. for $C_{46}H_{36}Hg_2N_{12}O_{12}$: C, 40.92; H, 2.69; N, 12.45%. Found: C, 40.64; H, 2.75; N, 12.55%. IR (KBr disk, cm^{-1}): 1615 (m), 1508 (m), 1465 (m), 1429 (m), 1384 (s), 1327 (m), 1281 (m), 1112 (m), 1031 (m), 839 (m), 776 (m), 618 (m), 546 (m) cm^{-1}. ^{1}H NMR (400 MHz, DMSO-d_6): δ = 8.76 (d, 4H, py), 8.30 (d, 4H, Ph), 8.12 (d, 4H, py), 7.95 (d, 2H, C=CH), 7.75 (m, 8H, Ph and py), 7.44 (d, 2H, C=CH), 7.17 (d, 4H, Ph), 7.12 (m, 4H, py), 7.01 (d, 4H, py).

X-Ray data collection and structure determination.

Single crystals of **1** and **2·H_2O·4MeCN** suitable for X-ray analysis were obtained directly from the above preparations. Intensity data for **1** and **2·H_2O·4MeCN** were collected either on a Rigaku-Oxford Diffraction Xcalibur/Gemini diffractometer with Atlas CCD detector using Mo-Kα (λ = 0.71073 Å) (**1**), or a Bruker APEX-II CCD diffractometer using Mo-Kα (λ = 0.71073 Å) (**2·H_2O·4MeCN**). Each single crystal was mounted on a glass fibre and data were collected at 223K for **1** and 273 K for **2·H_2O·4MeCN**. Data were integrated and unit cell parameters were determined using all observed reflections with the

program *CrysAlisPro* (Agilent Technologies, Version 1.171.36.32, 2013) for **1** and *APEX2* v2012.4-3 (Bruker, AXS) for **2**·H$_2$O·4MeCN. Absorption corrections (multi-scan) were applied by using the program *SADABS*.[65]

The crystal structures of **1** and **2**·H$_2$O·4MeCN were solved by direct methods and refined on F^2 by full-matrix least-squares methods with the *SHELXL-97* program.[68] All non-hydrogen atoms were refined anisotropically. For **1**, the vinyl group of the ppvppa ligand molecule was disordered over two positions and the occupancy factors were refined to 0.55(3)/0.45(3) for C17-C18/C1A-C2A. The 1,4-NDC ligands are disordered in two orientations with respect to a mirror plane. For **2**, the H$_2$O molecule sits within a cavity in the crystal structure and is disordered over two half-occupancy sites related by inversion symmetry. The water molecule forms O-H···π hydrogen bonds to two of the rings of a ppvppa ligand. A summary of crystallographic data for **1** and **2**·H$_2$O·4MeCN is given in Table 1.

Table 1 Summary of Crystallographic Data for **1** and **2**·H$_2$O·4MeCN

Compound	**1**	**2**·H$_2$O·4MeCN
Chemical formula	C$_{35}$H$_{24}$ZnN$_4$O$_4$	C$_{54}$H$_{50}$Hg$_2$N$_{16}$O$_{13}$
Formula weight	629.97	1532.28
Crystal system	triclinic	triclinic
Space group	$P\bar{1}$	$P\bar{1}$
a/Å	10.3894(5)	9.316(3)
b/Å	10.7374(5)	12.398(4)
c/Å	15.0526(8)	13.684(4)
α/°	97.447(4)	95.350(18)
β/°	97.813(4)	104.121(16)
γ/°	106.968(4)	102.151(18)
V/Å^3	1565.59(13)	1480.9(8)
Temperature/K	223(2)	273(2)
D_c/(g cm^{-3})	1.336	1.718
Z	2	1
μ (Mo-Kα)/mm^{-1}	0.829	5.253
F(000)	648	750
Total reflections	13250	56705
Unique reflections (R_{int})	6397 (0.040)	6816 (0.128)
No. reflns used in Refinement, n	6397	6816
No. parameters, p	562	385
Restraints, r	2	0
$R_1{}^a$	0.0694	0.0446
$wR_2{}^b$	0.2172	0.1006
GOF^c	1.050	1.113
$\Delta\rho_{max}/\Delta\rho_{min}$ (e Å^{-3})	1.176/-0.410	1.010/-1.232

$^a R_1 = \Sigma||F_o|-|F_c||/\Sigma|F_o|$. $^b wR_2 = [\Sigma w(F_o{}^2-F_c{}^2)^2/\Sigma w(F_o{}^2)^2]^{1/2}$. ^{c}GOF $= \{\Sigma[w((F_o{}^2-F_c{}^2)^2)]/(n+r-p)]\}^{1/2}$.

Spectroscopic measurements for Hg^{2+} sensing.

UV-Vis and fluorescence titrations were performed on 0.1 mM solutions of ppvppa in MeCN or suspensions of 0.1 mmol of **1** per litre of H$_2$O. Typically, aliquots of freshly prepared M(NO$_3$)$_n$ (M = Na$^+$, K$^+$, Zn^{2+}, Co^{2+}, Ni^{2+}, Cu^{2+}, Cd^{2+}, Mn^{2+}, Pb^{2+}, and Hg^{2+}) or MeHgI standard solutions (1.0 mM) in H$_2$O were added at room temperature, and then the UV-Vis and fluorescence spectra were recorded.

Acknowledgements

Notes and references

1 T. W. Clarkson and L. Magos, *Crit. Rev. Toxicol.*, 2006, **36**, 609.
2 W. Li and H. Tse, *Environ. Sci. Pollut. Res.*, 2015, **22**, 192.
3 H. R. Sunshine and S. J. Lippard, *Nucleic Acids Res.*, 1974, **1**, 673.
4 J. W. Sekowski, L. H. Malkas, Y. T. Wei and R. J. Hickey, *Toxicol. Appl. Pharmacol.*, 1997, **145**, 268.
5 I. Onyido, A. R. Norris and E. Buncel, *Chem. Rev.*, 2004, **104**, 5911.
6 B. N. Ahamed, M. Arunachalam and P. Ghosh, *Inorg. Chem.*, 2010, **49**, 4447.
7 A. X. Zheng, H. X. Li, K. P. Hou, J. Shi, H. F. Wang, Z. G. Ren and J. P. Lang, *Dalton Trans.*, 2012, **41**, 2699.
8 E. M. Nolan and S. J. Lippard, *Chem. Rev.*, 2008, **108**, 3443.
9 S. K. Pandey, K. H. Kim and R. J. C. Brown, *TrAC, Trends Anal. Chem.*, 2011, **30**, 899.
10 B. Dimitrova, K. Benkhedda, E. Ivanova and F. Adams, *J. Anal. At. Spectrom.*, 2004, **19**, 1394.
11 C. Locatelli, D. Melucci and G. Torsi, *Anal. Bioanal. Chem.*, 2005, **382**, 1567.
12 K. V. Meel, A. Smekens, M. Behets, P. Kazandjian and R. V. Grieken, *Anal. Chem.*, 2007, **79**, 6383.
13 L. Duan, Y. Xu and X. Qian, *Chem. Commun.*, 2008, 6339.
14 M. L. Ho, K. Y. Chen, L. C. Wu, J. Y. Shen, G. H. Lee, M. J. Ko, C. C. Wang, J. F. Lee and P. T. Chou, *Chem. Commun.*, 2008, 2438.
15 J. S. Kim and D. T. Quang, *Chem. Rev.*, 2007, **107**, 3780.
16 H. N. Kim, W. X. Ren, J. S. Kim and J. Yoon, *Chem. Soc. Rev.*, 2012, **41**, 3210.
17 S. Y. Ding, M. Dong, Y. W. Wang, Y. T. Chen, H. Z. Wang, C. Y. Su and W. Wang, *J. Am. Chem. Soc.*, 2016, **138**, 3031.
18 S. A. Rahaman, B. Roy, S. Mandal and S. Bandyopadhyay, *Inorg. Chem.*, 2016, **55**, 1069.
19 W. Jiang and W. Wang, *Chem. Commun.*, 2009, 3913.
20 X. Guo, X. Qian and L. Jia, *J. Am. Chem. Soc.*, 2004, **126**, 2272.
21 S. Y. Moon, N. R. Cha, Y. H. Kim and S. Chang, *J. Org. Chem.*, 2004, **69**, 181.
22 E. M. Nolan and S. J. Lippard, *J. Am. Chem. Soc.*, 2003, **125**, 14270.
23 K. D. Prasad, N. Venkataramaiah and T. N. G. Row, *Cryst. Growth Des.*, 2014, **14**, 2118.
24 Z. Shi, X. L. Tang, X. Y. Zhou, J. Cheng, Q. X. Han, J. A. Zhou, B. Wang, Y. F. Yang, W. S. Liu and D. C. Bai, *Inorg. Chem.*, 2013, **52**, 12668.
25 V. Bhalla, Roopa, M. Kumar, P. R. Sharma and T. Kaur, *Dalton Trans.*, 2013, **42**, 15063.
26 L. Shang, L. X. Yang, F. Stockmar, R. Popescu, V. Trouillet, M. Bruns, D. Gerthsen and G. U. Nienhaus, *Nanoscale*, 2012, **4**, 4155.

27 X. J. Liu, N. Zhang, T. Bing and D. H. Shangguan, *Anal. Chem.*, 2014, **86**, 2289.

28 Y. Qu, J. L. Hua and H. Tian, *Org. Lett.*, 2010, **12**, 3320.

29 D. Srikun, S. E. Miller, D. W. Domaille and C. J. Chang, *J. Am. Chem. Soc.*, 2008, **130**, 4596.

30 X. Peng, J. Du, J. Fan, J. Wang, Y. Wu, J. Zhao, S. Sun and T. Xu, *J. Am. Chem. Soc.*, 2007, **129**, 1500.

31 Y. Zhang, X. Guo, W. Si, L. Jia and X. Qian, *Org. Lett.*, 2008, **10**, 473.

32 K. Kiyose, H. Kojima, Y. Urano and T. Nagano, *J. Am. Chem. Soc.*, 2006, **128**, 6548.

33 Y. Kubo, M. Yamamoto, M. Ikeda, M. Takeuchi, S. Shinkai, S. Yamaguchi and K. Tamao, *Angew. Chem., Int. Ed.*, 2003, **42**, 2036.

34 M. Royzen, Z. Dai and J. W. Canary, *J. Am. Chem. Soc.*, 2005, **127**, 1612.

35 J. Zhou, C. Fang, T. Chang, X. Liu and D. Shangguan, *J. Mater. Chem. B*, 2013, **1**, 661.

36 D. W. Domaille, L. Zeng and C. J. Chang, *J. Am. Chem. Soc.*, 2010, **132**, 1194.

37 Y. Zhao, X. B. Zhang, Z. X. Han, L. Qiao, C. Y. Li, L. X. Jian, G. L. Shen and R. Q. Yu, *Anal. Chem.*, 2009, **81**, 7022.

38 W. Y. Lin, L. L. Long, B. B. Chen, W. Tan and W. S. Gao, *Chem. Commun.*, 2010, **46**, 1311.

39 Z. C. Wen, R. Yang, H. He and Y. B. Jiang, *Chem. Commun.*, 2006, 106.

40 Z. C. Xu, X. H. Qian and J. N. Cui, *Org. Lett.*, 2005, **7**, 3029.

41 Z. Yang, M. Y. She, B. Yin, J. H. Cui, Y. Z. Zhang, W. Sun, J. L. Li and Z. Shi, *J. Org. Chem.*, 2012, **77**, 1143.

42 L. Xue, Q. Liu and H. Jiang, *Org. Lett.*, 2009, **11**, 3454.

43 G. Q. Chen, Z. Guo, G. M. Zeng and L. Tang, *Analyst*, 2015, **140**, 5400.

44 M. Suresh, S. Mishra, S. K. Mishra, E. Suresh, A. K. Mandal, A. Shrivastav and A. Das, *Org. Lett.*, 2009, **11**, 2740.

45 J. J. Lee, Y. S. Kim, E. Nam, S. Y. Lee, M. H. Lim and C. Kim, *Dalton Trans.*, 2016, **45**, 5700.

46 X. L. Zhang, Y. Xiao, and X. H. Qian, *Angew. Chem., Int. Ed.*, 2008, **47**, 8025.

47 Y. P. Yang, X. L. Ni, T. Sun, H. Cong and G. Wei, *RSC Adv.*, 2014, **4**, 47000.

48 H. Xue, X. J. Tang, L. Z. Wu, L. P. Zhang and C. H. Tung, *J. Org. Chem.*, 2005, **70**, 9727.

49 S. M. Brombosz, A. J. Zucchero, R. L. Phillips, D. Vazquez, A. Wilson and U. H. F. Bunz, *Org. Lett.*, 2007, **9**, 4519.

50 L. Zhang and L. Zhu, *J. Org. Chem.*, 2008, **73**, 832.

51 X. J. Feng, P. Z. Tian, Z. Xu, S. F. Chen and M. S. Wong, *J. Org. Chem.*, 2013, **78**, 11318.

52 Q. Zhao, X. M. Liu, W. C. Song and X. H. Bu, *Dalton Trans.*, 2012, **41**, 6683.

53 Q. Zhao, R. F. Li, S. K. Xing, X. M. Liu, T. L. Hu and X. H. Bu, *Inorg. Chem.*, 2011, **50**, 10041.

54 Y. P. Li, Q. Zhao, H. R. Yang, S. J. Liu, X. M. Liu, Y. H. Zhang, T. L. Hu, J. T. Chen, Z. Chang and X. H. Bu, *Analyst*, 2013, **138**, 5486.

55 M. M. Chen, X. Zhou, H. X. Li, X. X. Yang and J. P. Lang, *Cryst. Growth Des.*, 2015, **15**, 2753.

56 Y. X. Shi, F. L. Hu, W. H. Zhang and J. P. Lang, *CrystEngComm*, 2015, **17**, 9404.

57 F. L. Hu, Y. X. Shi, H. H. Chen and J. P. Lang, *Dalton Trans.*, 2015, **44**, 18795.

58 M. M. Chen, H. X. Li and J. P. Lang, *Eur. J. Inorg. Chem.*, 2015, DOI: 10.1002/ejic.201501233.

59 J. J. Bergkamp, S. Decurtins and S. X. Liu, *Chem. Soc. Rev.*, 2015, **44**, 863.

60 S. Barlow, H. E. Bunting, C. Ringham, J. C. Green, G. U. Bublitz, S. G. Boxer, J. W. Perry and S. R. Marder, *J. Am. Chem. Soc.*, 1999, **121**, 3715.

61 G. E. Southhard and M. D. Curtis, *Organometallics*, 2001, **20**, 508.

62 K. Naka, T. Uemura and Y. Chujo, *Macromolecules*, 2000, **33**, 6965.

63 K. Gholivand, K. Farshadfer, S. M. Roe, A. Gholami and M. D. Esrafili, *CrystEngComm*, 2016, DOI: 10.1039/c5ce02208h.

64 B. V. Crist, Handbook of Monochromatic XPS Spectra: The Elements of Native Oxides, Wiley, Chichester, 2000.

65 G. M. Sheldrick, SADABS empirical absorption correction program,[66] University of Göttingen, based on the method of Blessing.[67]

66 L. Krause, R. Herbst-Irmer, G. M. Sheldrick and D. Stalke, *J. Appl. Cryst.*, 2014, **48**, 3.

67 R. H. Blessing, *Acta Crystallogr.*, 1995, **A51**, 33.

68 G. M. Sheldrick, *Acta Crystallogr.*, 2015, **C71**, 3.